

# High peak-to-valley current ratio $\text{In}_{0.53}\text{Ga}_{0.47}\text{As}/\text{AlAs}$ resonant tunneling diode with a high doping emitter\*

Wang Wei(王伟)<sup>1,2,†</sup>, Sun Hao(孙浩)<sup>1</sup>, Teng Teng(滕腾)<sup>1,2</sup>, and Sun Xiaowei(孙晓玮)<sup>1</sup>

<sup>1</sup>Key Laboratory of Terahertz Solid-State Technology, Shanghai Institute of Microsystem and Information Technology, Chinese Academy of Sciences, Shanghai 200050, China

<sup>2</sup>University of Chinese Academy of Sciences, Beijing 100039, China

**Abstract:** An  $\text{In}_{0.53}\text{Ga}_{0.47}\text{As}/\text{AlAs}$  resonant tunneling diode (RTD) with a high doping emitter is designed and fabricated using air bridge technology. The RTD exhibits a high peak-to-valley current ratio (PVCR) of more than 40 at room temperature, with a peak current density of  $24 \text{ kA}/\text{cm}^2$ . The extraction of device parameters from DC and microwave measurements is presented together with an RTD equivalent circuit. The high PVCR RTD with small intrinsic capacitance is favorable for microwave/THz applications.

**Key words:** resonant tunneling diode;  $I$ - $V$  characteristics; peak-to-valley current ratio; equivalent circuit;  $S$ -parameters

**DOI:** 10.1088/1674-4926/33/12/124002

**EEACC:** 2530C; 2560H

## 1. Introduction

Resonant tunneling diodes (RTDs) are promising devices for applications in microwave/THz and high-speed electronics, due to their built-in negative differential resistance (NDR) in non-linear  $I$ - $V$  characteristics. It has recently been reported that RTD oscillators can operate at over 1 THz at room temperature<sup>[1,2]</sup>. Moreover, RTDs have been integrated with heterojunction bipolar transistors (HBTs) or high electron mobility transistors (HEMTs) for high performance monolithic circuits<sup>[3,4]</sup>.

Peak current density and peak-to-valley current ratio (PVCR) are the two important figures of merit for RTDs. Generally, a thin barrier in an RTD can increase the peak current density, and a large conduction-band offset ( $\Delta E_C$ ) between the barrier and the well can improve the PVCR resulting from the reduction of the valley current<sup>[5]</sup>. Since  $\text{InGaAs}/\text{AlAs}$  material systems have the above characteristics, higher electron saturation velocity and lower electron effective mass, the performances of  $\text{InGaAs}/\text{AlAs}$  RTDs are much better than those of  $\text{GaAs}/\text{AlAs}$  ones, which are very attractive for researchers.  $\text{In}_{0.53}\text{Ga}_{0.47}\text{As}/\text{AlAs}/\text{InAs}$  RTDs have demonstrated a high peak-to-valley current ratio of 50 and a peak current density of  $5.8 \text{ kA}/\text{cm}^2$ <sup>[6]</sup>. Extremely high peak current densities of up to  $1 \times 10^6 \text{ A}/\text{cm}^2$  have been achieved in  $\text{InGaAs}/\text{AlAs}$  RTDs<sup>[7]</sup>.

In this paper, we present experimental results for the  $\text{In}_{0.53}\text{Ga}_{0.47}\text{As}/\text{AlAs}$  RTDs with a high doping emitter fabricated using air bridge technology. RTDs with a high PVCR of 43 and a peak current density  $24 \text{ kA}/\text{cm}^2$  at room temperature are demonstrated. The equivalent circuit model of the RTD is built, and its parameters are extracted from DC and microwave measurements. The RTDs show small intrinsic capacitance, which is advantageous for microwave/THz application.

## 2. RTD design and technology

The layer structure of  $\text{In}_{0.53}\text{Ga}_{0.47}\text{As}/\text{AlAs}$  RTDs was grown by molecular beam epitaxy (MBE) on 3-inch semi-insulating InP substrate. The epitaxial layer sequence is shown in Fig. 1. The intrinsic RTD structure consists of a double-barrier single-well (DBSW) structure with  $\text{AlAs}/\text{In}_{0.53}\text{Ga}_{0.47}\text{As}/\text{AlAs}$  (2 nm/4 nm/2 nm). In contrast to the InP-based RTDs presented in Refs. [8, 9], a high doping  $\text{In}_{0.53}\text{Ga}_{0.47}\text{As}$  emitter ( $2 \times 10^{18} \text{ cm}^{-3}$ , Si-doped) was applied to improve peak current density. To avoid the penetration of impurities from the doped emitter and collector to the DBSW region, un-doped spacer layers (5 nm) were grown between them. The spacer layers also effectively reduce ionized impurity scattering to improve the peak-to-valley current ratio (PVCR)<sup>[6,9]</sup>. Additionally, a thin heavy doping InP etch stop layer ( $1 \times 10^{19} \text{ cm}^{-3}$ , Si-doped) was inserted in the collector contact layer to effectively control the etch process. Prior to device fabrication, numerical simulations were carried out in order to predict the  $I$ - $V$  characteristics of RTDs<sup>[10]</sup>.

The InP-based RTDs in this work were fabricated using optical lithography, selective wet etching,  $\text{SiN}_x$  deposition, and metal lift-off technology. The process started with depositing a  $\text{SiN}_x$  film and creating  $15 \mu\text{m}$  diameter circular windows for definition of emitter electrodes. The emitter electrode ohmic contacts were formed by evaporating  $\text{Ge}/\text{Au}/\text{Ni}/\text{Au}$  and alloying at  $330 \text{ }^\circ\text{C}$  for 40 s. After dry etching  $\text{SiN}_x$  for collector contact windows and active mesas, the RTD-layer stack was selectively etched down to the lower InP layer by using a  $\text{H}_2\text{SO}_4 : \text{H}_2\text{O}_2 : \text{H}_2\text{O} = 1 : 1 : 20$  solution. Slight over-etching of the wafer ensures etch depth uniformity. Then the InP etch stop layer was quickly removed using an solution of  $\text{HCl} : \text{H}_3\text{PO}_4 = 1 : 3$ . Since the collection contact layer is heavily-doped  $\text{In}_{0.53}\text{Ga}_{0.47}\text{As}$ , non-alloyed ohmic contacts (Ti/Au) were used.

\* Project supported by the National Fundamental Research Program of China (No. 2009CB320207).

† Corresponding author. Email: wangwei@mail.sim.ac.cn

Received 26 April 2012, revised manuscript received 3 July 2012

E- electrode (Ge/Au/Ni/Au)		
$n^+-\text{In}_{0.53}\text{Ga}_{0.47}\text{As}$	$1 \times 10^{19} \text{ cm}^{-3}$	100 nm
Emitter contact		
$n-\text{In}_{0.53}\text{Ga}_{0.47}\text{As}$	$2 \times 10^{18} \text{ cm}^{-3}$	40 nm
Emitter		
$i-\text{In}_{0.53}\text{Ga}_{0.47}\text{As}$		5 nm
Spacer		
$i-\text{AlAs}$		2 nm
Barrier		
$i-\text{In}_{0.53}\text{Ga}_{0.47}\text{As}$		4 nm
Well		
$i-\text{AlAs}$		2 nm
Barrier		
$i-\text{In}_{0.53}\text{Ga}_{0.47}\text{As}$		5 nm
Spacer		
$n-\text{In}_{0.53}\text{Ga}_{0.47}\text{As}$	$2 \times 10^{18} \text{ cm}^{-3}$	40 nm
Collector		
$n^+-\text{InP}$	$1 \times 10^{19} \text{ cm}^{-3}$	3 nm
Etch stop		
$n^+-\text{In}_{0.53}\text{Ga}_{0.47}\text{As}$	$1 \times 10^{19} \text{ cm}^{-3}$	400 nm
C- electrode (Ti/Au)		
Collector contact		
$i-\text{In}_{0.53}\text{Ga}_{0.47}\text{As}$		200 nm
SI-InP		

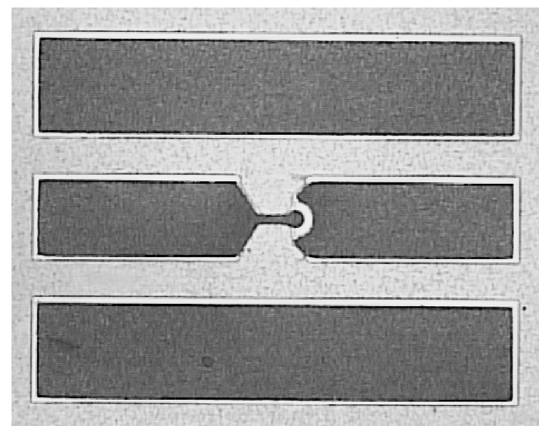
Fig. 1. Layer sequence and structure of the  $\text{In}_{0.53}\text{Ga}_{0.47}\text{As}/\text{AlAs}$  RTD.

In order to form coplanar waveguide (CPW) electrodes connecting to devices, a 3- $\mu\text{m}$ -thick gold layer was electroplated in the CPW electroplating mold. After active areas and electrodes were protected by a photoresist, the wafer was etched down to the semi-insulating InP substrate for device isolation. An emitter air-bridge connection was fabricated finally by means of lateral wet etching of the epitaxial layers underneath the bridge to form an air cavity. The air-bridge structure can reduce the parasitic capacitance and improve the high-frequency performance of an RTD. Figure 2(a) shows an optical micrograph of the fabricated RTD with CPW electrodes. Figure 2(b) is an SEM image of the air-bridge structure.

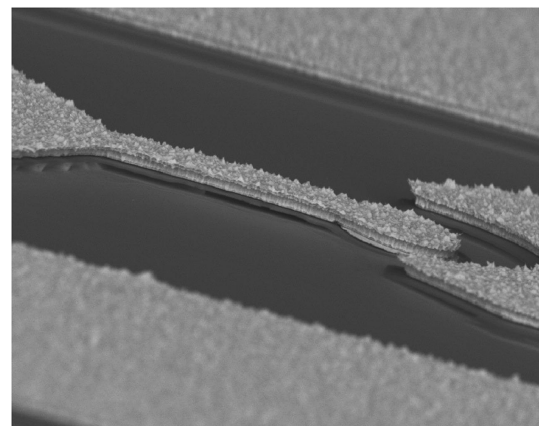
### 3. Device characterization and discussion

The  $\text{In}_{0.53}\text{Ga}_{0.47}\text{As}/\text{AlAs}$  RTDs were measured on-wafer at room temperature. The DC characteristics of the RTDs were measured with an HP4156A semiconductor parameter analyzer. The  $I-V$  curve of the fabricated RTDs with an emitter area of  $\pi \times (15/2)^2 \mu\text{m}^2$  is given in Fig. 3. The peak current is 43 mA, which corresponds to a peak current density of 24  $\text{kA}/\text{cm}^2$ . The valley current is close to 1 mA. So the peak-to-valley current ratio is greater than 43. The plateau-like structure in the  $I-V$  curve is due to the formation of the emitter quantum well (EQW) and the coupling of its quasi-bound state to the state in the main quantum well (QW)<sup>[11]</sup>.

The high PVCR of RTDs can be largely related to the weak scattering in the  $\text{In}_{0.53}\text{Ga}_{0.47}\text{As}$  well. The small scattering potential in the DBSW structure can decrease valley current density significantly and increase peak current density slightly, resulting in a dramatic improvement in the PVCR, which is demonstrated by numerical simulation results using a non-equilibrium Green's function<sup>[10]</sup> or the Wigner function model<sup>[11]</sup>. In the multilayer device structure, the un-doped spacer layers next to the DBSW contribute to reduce scatter-



(a)



(b)

Fig. 2. (a) Micrograph of the fabricated RTD with CPW electrodes. (b) SEM image of the air-bridge structure.

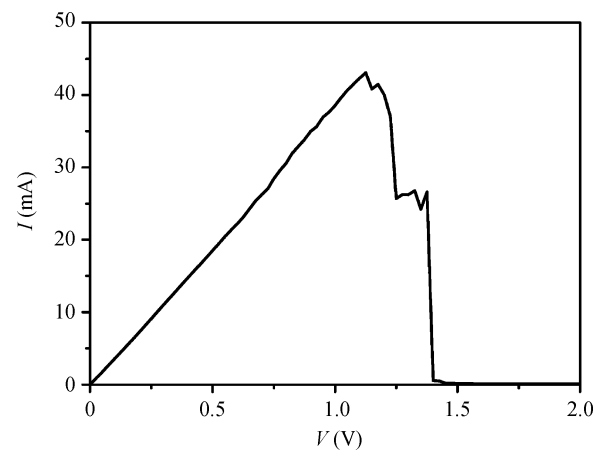


Fig. 3.  $I-V$  curve of a 15  $\mu\text{m}$  diameter circular RTD at room temperature.

ing from the high doping emitter and collector. Moreover, a high conduction-band offset ( $\Delta E_C$ ) between the AlAs barrier and the  $\text{In}_{0.53}\text{Ga}_{0.47}\text{As}$  well can effectively reduce valley current density by suppressing the thermionic electron transport at room temperature.

Besides the PVCR, the peak current density is also an important figure of merit for RTDs. The peak current density mea-

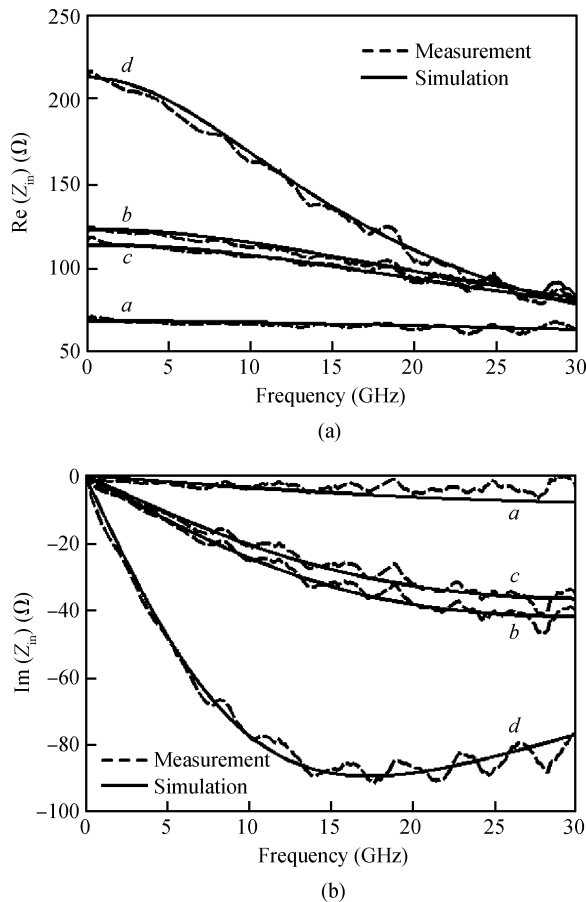


Fig. 4. Simulated input impedances compared with measurements. (a) Real parts of impedance. (b) Imaginary parts of impedance.

sured in this work is not high enough because the AlAs barrier is too thick (2 nm), in spite of the use of a highly doped emitter. The peak current density is determined by the epitaxial layer structure of the RTD, with the most critical component being the exponential dependence on the thickness of barrier layers<sup>[5]</sup>. Following reduction of the thickness of AlAs layers to six or five monolayers (1.7 nm or 1.4 nm) and adjusting layer structure parameters slightly, we think that a better RTD with high PVCR and high peak current density could be attained for microwave application.

The two-port *S*-parameters of the RTDs were measured with an Agilent N5245A vector network analyzer from 100 MHz to 30 GHz. The test port power was set to -20 dBm. The bias voltage was applied to the device through the internal bias-tees of N5245A. The system was calibrated with a short-open-load-through calibration standard. Figure 4 shows the measured input impedances for a RTD biased at (a) pre-peak, (b) near-peak, (c) plateau, and (d) valley voltage points, respectively.

The proposed RTD equivalent circuit (EC) model is shown in Fig. 5.  $R_S$  here represents the contact resistance and bulk resistance.  $C_D$  represents the total RTD capacitance including both the geometrical depletion capacitance and the quantum capacitance.  $R_D$  represents the differential resistance and is associated with the  $I-V$  behavior of the RTD. The extrinsic elements,  $R_P$ ,  $L_P$  and  $C_P$  are used to describe the impedance of contact pads and connecting conductors<sup>[12]</sup>.

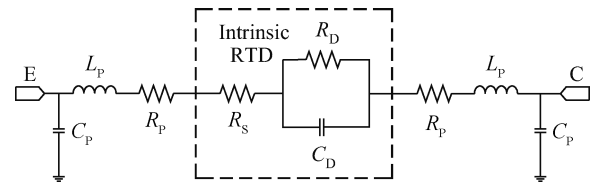


Fig. 5. Equivalent circuit model of the RTD with CPW electrodes.

The simulations using the proposed EC model are shown in Fig. 4, which are in good agreement with the measurements. The extracted capacitance  $C_D$  is found to be between 0.05 to 0.22 pF, which is the result of the variation of depletion width and well charge with bias voltage<sup>[13]</sup>. The  $R_S$  is bias-independent and closely equals to 2  $\Omega$ . The  $R_D$  describes the DC behavior and is negative in the NDR bias range. The  $R_D$  can be obtained by differentiating the  $I-V$  curve of the RTD, which is approximately equal to -8  $\Omega$ . The resistive cut-off frequency  $f_R$  of the intrinsic RTD can be calculated by<sup>[8]</sup>

$$f_R = \frac{1}{2\pi |R_D| C_D} \sqrt{\frac{|R_D|}{R_S} - 1}. \quad (1)$$

Using the extracted parameters, we can roughly estimate that the resistive cut-off frequency is over 150 GHz.

According to Eq. (1), the RTD capacitance  $C_D$  is the most important factor to improve the resistive cut-off frequency  $f_R$ . Higher cut-off frequency  $f_R$  will be possible by further decreasing the mesa area and optimizing the structure of RTD. In addition, reducing the negative resistance  $R_D$  value can effectively improve the  $f_R$  of the RTD. Therefore, the high peak current density and the high PVCR of the RTD will help to achieve an increase of the resistive cut-off frequency  $f_R$  by reducing the negative resistance  $R_D$ .

#### 4. Conclusion

The  $\text{In}_{0.53}\text{Ga}_{0.47}\text{As}/\text{AlAs}$  RTD epitaxial layer structure with a high doping emitter has been designed and grown on InP substrate by MBE. The RTDs with a high peak-to-valley current ratio (PVCR) of more than 40 and a peak current density 24  $\text{kA}/\text{cm}^2$  at room temperature have been successfully fabricated using air bridge technology. The equivalent circuit model parameters have been extracted from DC and microwave measurements. The resistive cut-off frequency of an intrinsic RTD is estimated to be greater than 150 GHz. The experiment lays a foundation for the development of high-performance RTDs and their application in mm-wave/THz.

#### References

- [1] Feiginov M, Sydlo C, Cojocari O, et al. Resonant-tunnelling-diode oscillators operating at frequencies above 1.1 THz. *Appl Phys Lett*, 2011, 99(23): 233506
- [2] Suzuki S, Asada M, Teranishi A, et al. Fundamental oscillation of resonant tunneling diodes above 1 THz at room temperature. *Appl Phys Lett*, 2010, 97(24): 242102
- [3] Huang Yinglong, Ma Long, Yang Fuhua, et al. Resonant tunnelling diodes and high electron mobility transistors integrated on GaAs substrates. *Chinese Physics Letters*, 2006, 23(3): 607

- [4] Sunkyu C, Yongsik J, Kyoungsoon Y. Low DC-power Ku-band differential VCO based on an RTD/HBT MMIC technology. *IEEE Microw Wireless Compon Lett*, 2005, 15(11): 742
- [5] Miyamoto Y, Tobita H, Oshima K, et al. Barrier thickness dependence of peak current density in GaInAs/AlAs/InP resonant tunneling diodes by MOVPE. *Solid-State Electron*, 1999, 43(8): 1395
- [6] Smet J H, Broekaert T P E, Fonstad C G. Peak-to-valley current ratios as high as 50 : 1 at room temperature in pseudomorphic In<sub>0.53</sub>Ga<sub>0.47</sub>As/AlAs/InAs resonant tunneling diodes. *J Appl Phys*, 1992, 71(5): 2475
- [7] Sugiyama H, Yokoyama H, Teranishi A, et al. Extremely high peak current densities of over  $1 \times 10^6$  A/cm<sup>2</sup> in InP-based InGaAs/AlAs resonant tunneling diodes grown by metal-organic vapor-phase epitaxy. *Jpn J Appl Phys*, 2010, 49(5): 051201
- [8] Qi Haitao, Feng Zhen, Li Yali, et al. Fabrication of a high-performance RTD on InP substrate. *Chinese Journal of Semiconductors*, 2007, 28(12): 1945
- [9] Han Chunlin, Chen Chen, Zou Penghui, et al. InP-base resonant tunneling diodes. *Journal of Semiconductors*, 2009, 30(6): 064001
- [10] Wang Wei, Sun Hao, Sun Xiaowei, et al. Numerical simulation on characteristics of InP-base resonant tunneling diode. *Research & Progress of SSE*, 2010, 30(3): 317
- [11] Zhao P, Cui H L, Woolard D L, et al. Equivalent circuit parameters of resonant tunneling diodes extracted from self-consistent Wigner-Poisson simulation. *IEEE Trans Electron Devices*, 2001, 48(4): 614
- [12] Alkeev N V, Velling P, Khorenko E, et al. Resonant tunneling diode impedance dependence analysis. *MSMW04 Symposium Proceedings, Kharkov, Ukraine, 2004*: 566
- [13] Janes D B, Webb K J, Carroll M S, et al. Direct current and microwave characterization of integrated resonant tunneling diodes. *J Appl Phys*, 1995, 78(11): 6616